

PREPARED FOR THE U.S. DEPARTMENT OF ENERGY,
UNDER CONTRACT DE-AC02-76CH03073

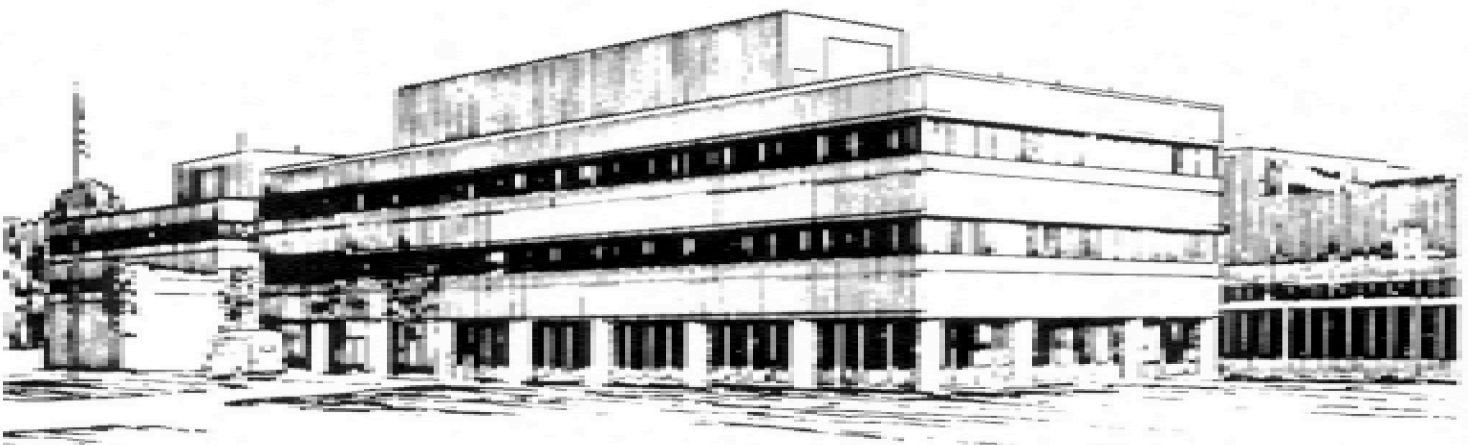
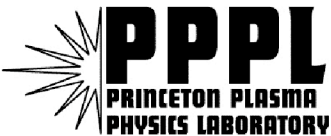
PPPL-4009
UC-70

PPPL-4009

**Structural Analysis
of the NCSX Vacuum Vessel**
by

Fred Dahlgren, Art Brooks, Paul Goranson,
Mike Cole, and Peter Titus

September 2004



**PRINCETON PLASMA PHYSICS LABORATORY
PRINCETON UNIVERSITY, PRINCETON, NEW JERSEY**

PPPL Reports Disclaimer

This report was prepared as an account of work sponsored by an agency of the United States Government. Neither the United States Government nor any agency thereof, nor any of their employees, makes any warranty, express or implied, or assumes any legal liability or responsibility for the accuracy, completeness, or usefulness of any information, apparatus, product, or process disclosed, or represents that its use would not infringe privately owned rights. Reference herein to any specific commercial product, process, or service by trade name, trademark, manufacturer, or otherwise, does not necessarily constitute or imply its endorsement, recommendation, or favoring by the United States Government or any agency thereof. The views and opinions of authors expressed herein do not necessarily state or reflect those of the United States Government or any agency thereof.

Availability

This report is posted on the U.S. Department of Energy's Princeton Plasma Physics Laboratory Publications and Reports web site in Fiscal Year 2004. The home page for PPPL Reports and Publications is: http://www.pppl.gov/pub_report/

DOE and DOE Contractors can obtain copies of this report from:

U.S. Department of Energy
Office of Scientific and Technical Information
DOE Technical Information Services (DTIS)
P.O. Box 62
Oak Ridge, TN 37831

Telephone: (865) 576-8401

Fax: (865) 576-5728

Email: reports@adonis.osti.gov

This report is available to the general public from:

National Technical Information Service
U.S. Department of Commerce
5285 Port Royal Road
Springfield, VA 22161

Telephone: 1-800-553-6847 or
(703) 605-6000

Fax: (703) 321-8547

Internet: <http://www.ntis.gov/ordering.htm>

Structural Analysis of the NCSX Vacuum Vessel

Fred Dahlgren, Art Brooks, PPPL, PO Box 451, Princeton NJ,08543
Paul Goranson, Mike Cole, ORNL, PO Box 2008 MS6169, Oak Ridge TN 37831-6169
Peter Titus, MIT Plasma Science and Fusion Center, 185 Albany Street Cambridge Ma. 02139

Abstract

The NCSX vacuum vessel has a rather unique shape being very closely coupled topologically to the three-fold stellerator symmetry of the plasma it contains. This shape does not permit the use of the common forms of pressure vessel analysis and necessitates the reliance on finite element analysis. The current paper describes the NCSX vacuum vessel stress analysis including external pressure, thermal, and electro-magnetic loading from internal plasma disruptions and bakeout temperatures of up to 400 degrees centigrade. Buckling and dynamic loading conditions are also considered.

I. Introduction

NCSX (National Compact Stellerator Experiment) is a DOE sponsored plasma physics experiment¹ being built at PPPL (the Princeton University Plasma Physics Laboratory) in Princeton NJ. The primary goal of this experiment is to explore the behavior of magnetically confined plasmas in a compact stellerator geometry. The interest in this magnetic topology is based largely on the expected inherent stability of plasmas confined in this way.

The focus of this paper is to describe the analysis of the stresses, displacements, and structural stability of the vacuum vessel shell, ports, and structural support attachments in response to various anticipated loading conditions and to verify the adequacy of the current design for the NCSX experiment.

The main vessel shell is to be fabricated from 0.375" thick Inconel-625 plate with port wall thicknesses varying from 0.125" to 0.5" depending on port diameter and configuration. The three 120 degree shells will be fabricated by welding together individually formed segments of Inconel plate and the three closure welds will be performed at final machine assembly.

Several anticipated loading conditions were investigated including external atmospheric pressure, gravity, thermal loads due to bakeout and normal operations, disruption eddy current loads, and seismic loading conditions.

II. FEA Model Description:

The vacuum vessel, modular coils (that produce the predominant magnetic fields), and the plasma, all have a closely coupled three-fold cyclic symmetry about the vertical axis of the machine. Figure 1. at the right shows the basic 120 degree single period FEA model of the vessel with cyclic-symmetric boundary conditions (multipoint

constraints in Nastran). Below is a list of the model details and loading conditions investigated:

Model Details:

38,906 DOF's
7782 GRID POINTS
7,228 CQUAD4
1,018 CTRIA3
40 MPC's
4 SPC's

Boundary Conditions:

Cyclic-Symmetry @ welded edge
via MPC's, vertically fixed @ top
clevis, circumferentially top & bot.
of NB port

Normal Operating Loads:

Uniform external 14.7 psi
Gravity – 1g
Temperature 200 deg.C (max.)
Bakeout: 400 deg.C (max)

Off-Normal (EM Disruption) Loads:

320kA Plasma @ 1.7T
210kA Plasma @ 2.0T (High Beta)
320kA Plasma @ 1.7T @dZ=10cm
(Inductively coupled solutions)

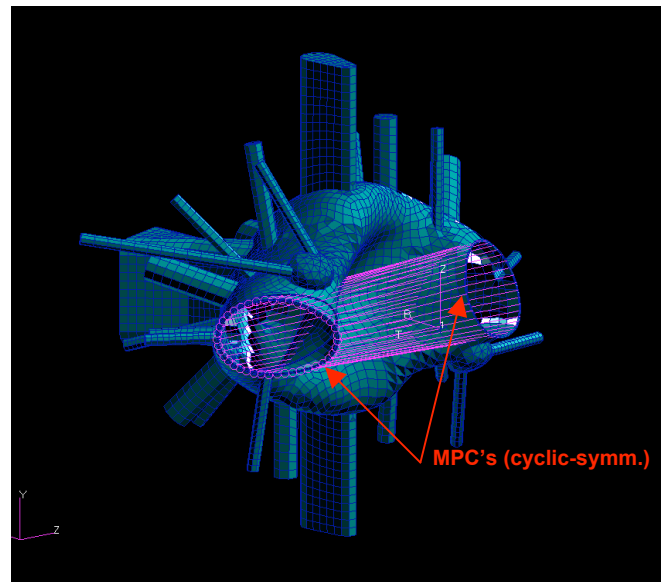


Figure 1. NCSX Vacuum Vessel FEA Model

The FEA code used in these analysis was MSC/Nastran – 2001-rev3 –Windows edition. The disruption loading was calculated using the PPPL code Spark ver.20b. Seismic and verification runs were made using Ansys Release 7.0.

Due to the very complex nature of the NCSX geometry it was necessary to model the vessel and other device components using a CAD (Computer Aided Design) program which relied on input from mathematically defined and generated surfaces. The vessel and coil shapes were dictated by the magnetic surfaces required on the plasma boundary. Pro-E was used for the CAD modeling and the main vessel geometry and ports were exported via Iges files which could be read by MSC/Patran (the modeling front-end and post processor for Nastran). The FEA model itself was generated and meshed in Patran from these surfaces, and is comprised of triangular and quadrilateral shell elements (CQUAD4 & CTRIA3) which include both bending and membrane stiffness.

II. Loading Conditions:

The main loads of consequence acting on the vessel are gravity, the external atmospheric load, thermal gradients during bakeout and normal operations, and Lorentz forces produced by electromagnetic interaction with the eddy currents induced during plasma disruptions. Three different disruption loading conditions were assumed, a stationary disruption of a 350kA plasma in a 1.7 Tesla field after being vertically displaced 10 cm, a stationary disruption of a 210 kA plasma in a 2 Tesla field in it's nominal mid-plane position (a high-beta configuration), and a 350kA plasma current in it's nominal position in a 1.7 Tesla field.

The uniform external atmospheric load was applied to the shell elements as pressures (PLOAD4 in Nastran apportions pressure loads to the element grid points via the element shape functions). The disruption loads were applied directly to the grid points via 3D force vectors. Nastran calculates gravity vector forces on element grid points by using the appropriate product of density and proportional volume associated with each node and using the specified acceleration direction and magnitude. Thermal loads are applied by specifying grid point temperatures and the strain free default temperature.

Although Princeton NJ is in a relatively stable earthquake zone, accelerations due to seismic events were also considered and are reported on elsewhere in these proceedings.²

III. FEA Stress Results:

Figure 2. is a contour plot of displacements due to a 1 atmosphere pressure loading condition (ie. during normal operation). The peak displacement is seen to be of 0.25” at the upper and lower ends of port-2 (at the 1st port flange). The deflection of ports 2 (and 9) are the result of a local inward displacement of the vessel shell in the flat area of the shell in the vicinity of these two ports as shown in Figure 3 (note the upper range of the contour levels in this plot has been limited to 0.125” to accentuate the local displacement

contours). Figure 4. shows the Tresca stress contours on the outer shell surface for atmospheric loading with the peak stress of 15.2 ksi occurring in the areas of highest curvature near the top (and bottom) of the shell.

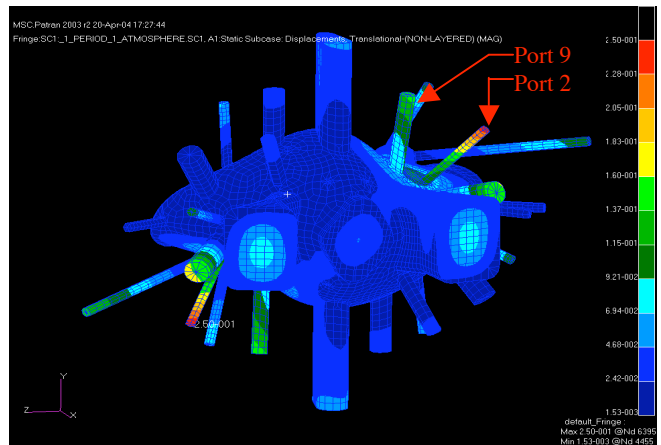


Figure 2. Displacements - Atmospheric Pressure Only

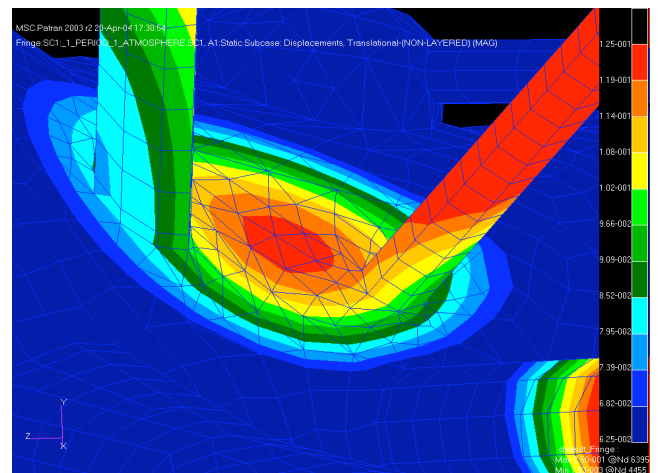


Figure 3. Displacements - Atmospheric Pressure Only

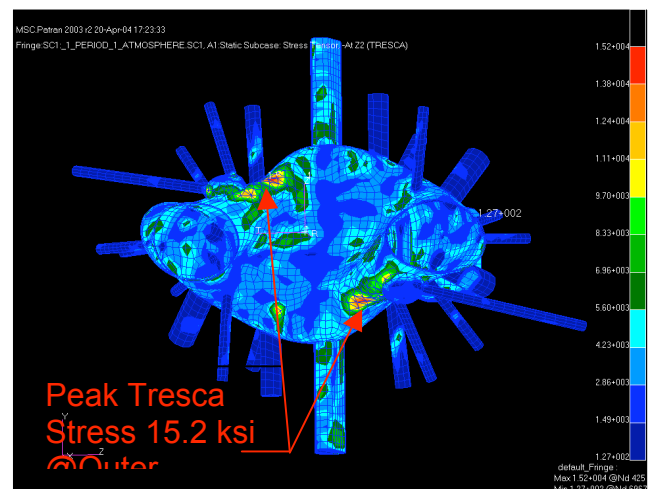


Figure 4. Tresca Stress - Atmospheric Pressure Only

The allowable stress intensity (Tresca stress) for 400 °C Inconel-625, per the ASME BPVC (Boiler & Pressure

Vessel Code), is 30.4 ksi (209.6 MPa). These values are nominally based on the 1/3rd minimum ultimate or 2/3rd minimum yield stress specified for this material at temperature, and indicate a comfortable margin for normal operations.

Figure 5. is a vector plot of applied forces from a VDE (Vertical Disruption Event). The main eddy currents in the shell during plasma disruptions generally flow around the vessel mid-plane on the inner wall as can be seen by the concentration of forces there. Figure 6. is a contour plot of the Tresca stresses resulting from a combined loading condition which includes atmospheric, gravity, and the VDE EM disruption forces.

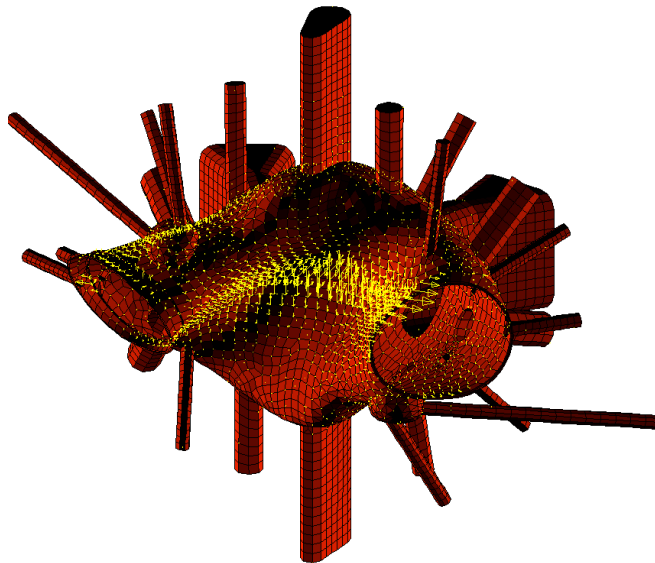


Figure 5. EM Self Forces on the Vessel Due to a VDE Disruption Loading.

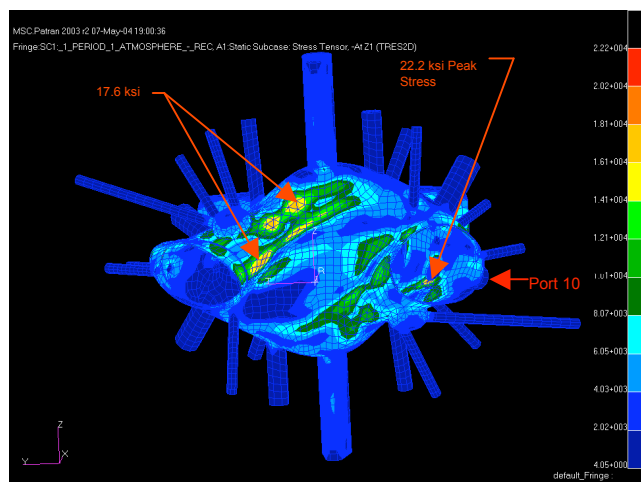


Figure 6. Tresca Stress Contours for a VDE + Atmosphere + Gravity Loading Condition.

The peak stress of 22.2 ksi (153 MPa) is a localized stress and is seen to occur at the lower intersection of the Port 10

nozzle with the shell, with the stress in the high curvature region of the shell peaking at 17.7 ksi (121.3 MPa).

Table I below summarizes the results for the various loading conditions investigated and compares those results to B.P.V.C. code allowable stress:

Loading	Peak Stress Intensity ksi (MPa)	Stress Category (per ASME BPVC)	Weld Efficiency No Rad. Insp.	Allowable Stress (ksi) for category	Safety Margin (above Allow.)	Notes
Press.	16.1 (111.0)	PL + Pb	0.7 -> 23.0ksi	1.5 x S _m (50.1)	2.1	@Turret
Press. + Grav.	15.7 (108.3)	PL + Pb	0.7 -> 22.4ksi	1.5 x S _m (50.1)	2.1	@Turret
Press. + Grav. + 500lb Cant.	34.3 (236.4)	PL +Pb + Q	0.5 -> 68.6ksi	3.0 x S _m (100.2)	1.4	@Turret RF-1 Administratively controlled
Ohmic Disrupt. 320kA-1.7T(+P+G)	17.7 (122.0)	PL + Pb	0.7 -> 25.3ksi	1.5 x S _m (50.1)	2.0	@Turret DLF = 1.0 (s/b less ~ 0.12)
Hi-Beta Disrupt. 210kA-2.0T(+P+G)	16.1 (111.0)	PL + Pb	0.7 -> 23.0ksi	1.5 x S _m (50.1)	2.1	@weld flange DLF = 1.0 (s/b less ~ 0.12)
VDE Disrupt. (+P+G) 320kA-1.7T-10cm	27.6 (190.3)	PL + Pb	0.7 -> 39.4ksi	1.5 x S _m (50.1)	1.2	@weld flange DLF = 1.0 (s/b less ~ 0.12)
Press. + Grav. +Thermal 400 C	31.0 (213.7)	PL + Pb + Q	0.5 -> 62.0	3.0 x S _m (100.2)	1.6	@NB-Port Excessive gradient assumed

Appendix 4, Section VIII – Division 2 the general stress criteria and categories for vessel design based on stress analysis can be found in Table II below:

Category	Description	Not to exceed
P _m	Primary membrane Stress (Average across solid section, produced only by body forces and mechanical loads).	1.0k x S _m
PL	Local Primary membrane Stress (Average stress across section, includes discontinuities but not Stress concentrations).	1.5k x S _m *
P _b	Primary bending stress (Stresses proportional to the distance from the centroid of a solid section – excludes discontinuities & str.conc.).	1.5k x S _m *
Q	Secondary Membrane + bending stresses, self equilibrating, due to thermal or mechanical loads, or discontinuities (excludes local stress concentrations).	3.0k x S _m **
F	Incremental stress added by stress concentrations (notch), thermal stresses producing thermal fatigue.	NA

* P_l or P_l + P_b < 1.5k x S_m, (k typically = 1.0),
 ** P_l + P_b + Q < 3.0k x S_m (stress intensity range)

Applying the Pressure vessel code criteria, which includes a knock down factor to the allowable stress intensity for weld efficiency, the minimum margin for all loading conditions considered, was 1.2 for the combined loading VDE case. Since disruption loads will be applied over a relatively short period (~1 to 30 msec.), the dynamic loading factor must be considered. In general if the applied load frequency is significantly different from natural frequency of the structure the DLF (Dynamic Load Factor) will be less than 1.0. To determine the natural frequency of the vessel, a modal analysis was run and the primary undamped natural

period of 1.25 seconds, was found to be a rocking mode with the inner and outer portions of the shell moving vertically in opposite directions with the motion centered around the vertical supports. Based on the ratio of periods between the natural frequency of the vessel and VDE disruption loading, the DLF was determined to be ~0.14 indicating that only a small fraction of the dynamic load will actually produce a response in the vessel structure. Higher order modes might involve many of the cantilevered ports, but since the dynamic portion of the loading is almost exclusively in the shell, the VDE will have little or no effect on the ports.

IV. Structural Stability:

To determine the structural stability of the vessel due to the external pressure and disruption loads, a buckling analysis was performed. In Nastran the common method of determining structural stability is to apply the loading conditions anticipated in normal service as a static loading condition and from that result calculate the differential stiffness matrix and then solve the resulting eigenvalue problem below:

$$[K + \lambda K_d] \{u\} = 0$$

The resulting (primary) eigenvalue is then the factor by which the applied load must be multiplied to produce buckling. If the original static load applied is one atmosphere the resulting eigenvalue is then the critical buckling load factor or safety factor.

For a single external atmospheric load (14.7 psi), the critical buckling load factor was found to be 12.99 indicating it would theoretically require approximately 191 psi external pressure to collapse the vessel (the resulting eigenvector seen in figure 7 shows the primary buckling mode shape). While 12.99 appears to be quite a large margin such results are typically viewed with some caution. The ASME-BPV code generally requires minimum safety factors of 5x or greater on critical buckling of externally loaded vessels due to the uncertainties in geometry, loading conditions, and material properties. Regularly shaped structures commonly used in autoclaves, like spheres, torrispherical heads and cylindrical shells, tend to be more sensitive to variations in thickness and deviations from their theoretical geometry and tend to buckle at loads significantly lower than normal stability theory might predict (hence the large safety factors of 5x or greater), however, due to the highly irregular shape of the NCSX vessel, it is less likely to be susceptible to premature buckling due to minor variations in thickness or geometry.

That said there are still other considerations that tend to produce lower buckling margins than this eigenvalue analysis predicts, and suggests these margins should only be used as an upper bound indicator of global structural stability. There are several assumptions inherent in the current method of buckling analysis, the principle one being that the entire structure at temperature and under load remains linearly elastic and therefore small deflection

theory still applies (ie. the applied loads from which the differential stiffness is derived, maintain the same magnitude, direction, and point of application as the structure deflects).

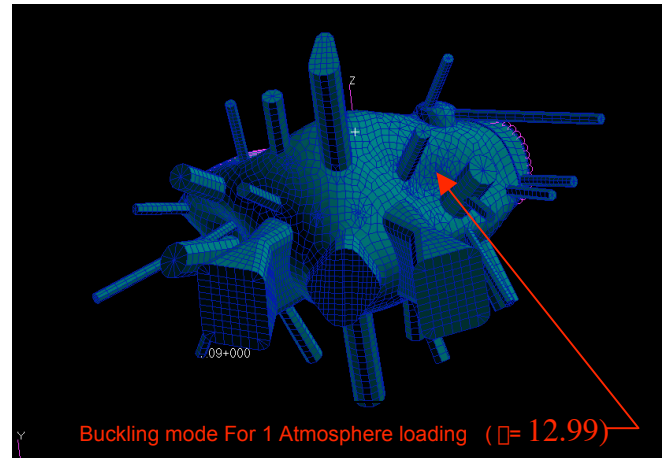


Figure 7. Primary Buckling Mode Shape

Figure 8 is a contour plot of Tresca stresses that exceed the yield stress of Inconel-625 at 400 deg.C (~60 ksi) when a full 191 psi (12.99 x 14.7 psi) external load is applied. Clearly, these localized areas of high stress would have yielded, producing large shell displacements, long before a 191 psi pressure was reached, so the safety factor quoted above of 12.99 is not necessarily a true indicator of the margin for structural failure.

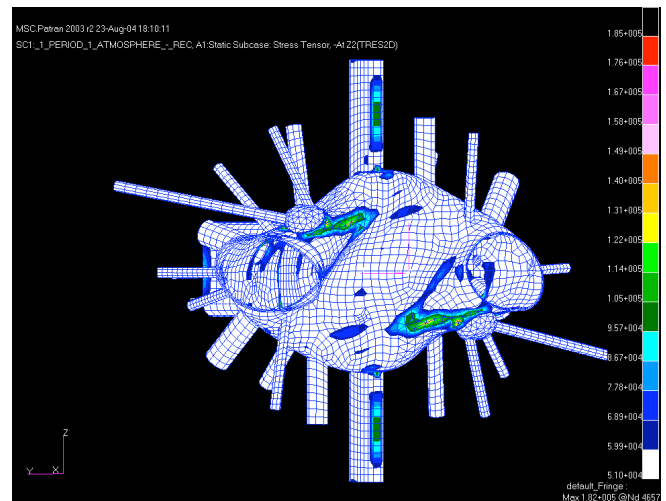


Figure 8. Stresses exceeding yield for 12.99 Bar Loading

Figure 9 is a Tresca stress contour plot for a 5x atmospheric (73.5 psi) loading condition. It can be seen that only a very small region of the shell at the corner intersection with the rectangular ports exceeds yield and it therefore can be concluded that only localized yielding and small displacements would occur under these loading conditions. The main conclusion that can be drawn from these results is that the buckling margin, at a minimum, exceeds 5x for atmospheric loading at the maximum bakeout temperature.

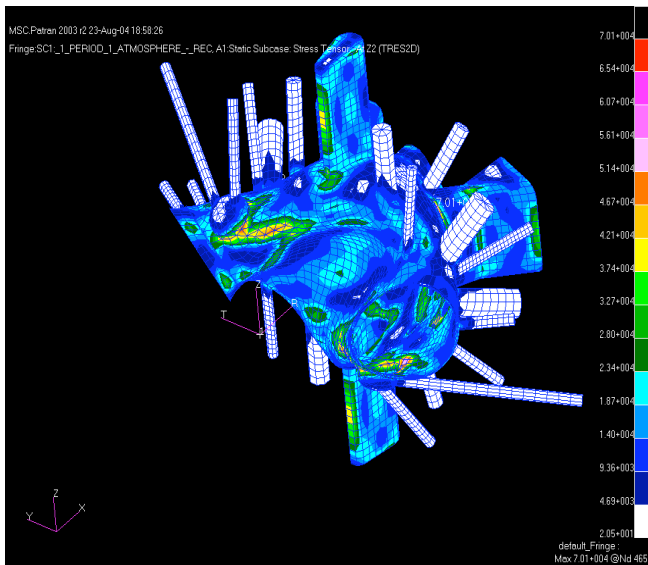


Figure 9. Stresses for 5 Bar Loading ($S_{Tresca} < S_{yield}$)

V. Discussion and Conclusions:

The purpose of this analysis was to determine the stresses, displacements, and structural stability of the vacuum vessel shell, ports, and structural support attachments in response to various loading conditions and to verify the adequacy of the current design. Several anticipated loading conditions were investigated including external atmospheric pressure, gravity, thermal loads due to bakeout and normal operations, disruption eddy current loads, and seismic loading conditions. The following are the main findings of this analysis:

-Stresses from the normal operating load runs (Atmospheric, Gravity, Thermal, + 250 lb cantilevered load) in the shell and ports are generally well below the code allowable stress with the exception of the Port-18 & 15 cantilevered loading condition. Recommend either:

- thickening the turret wall and port nozzle to reduce stress at the nozzle/porter section and to reduce vertical deflections of the port,
- Implement a radially compliant vertical nozzle support off the cryostat, or
- Limit the cantilevered loading on Port-15 and the RF ports.

-Shell displacements for normal operations are generally low with the exception of the area between Port-2 & Port-9 which indicate a displacement of 0.125" total. This results in a .25" deflection of these ports at the 1st flange. These displacements may be reduced by thickening or reinforcing the shell locally to reduce these deflections if necessary.

-Dynamic loading from VDE (10cm vertically displaced) plasma disruptions are the most severe but the peak (Main flange) stress intensities are below allowables for the full 1.0x DLF (Dynamic Load Factor). Where we assume the interior welds in the peak stress (flange) regions experience

the same stresses, and using a weld efficiency of 0.7, we have a margin of 20% on code allowables.

-Critical Buckling loads for the worst VDE disruption load (using DLF=1.0) and including atmospheric and gravity loading, the critical load factor was 12. Due to the irregular shape of this vessel local buckling modes predominate, generally localized in the shell near ports 2 and 9. The current design has a buckling margin > 5.

-Modal analysis indicates the undamped primary structural mode of 0.8 Hz with the vessel rocking on the vertical supports. Numerous low frequency modes are present in ports 15, 2, 9, rf-1 & rf-2. Several are in the frequency range of earthquake spectrum and are anticipated to participate in the horizontal and vertical accelerations of any seismic event. Since their mass is relatively low, and deflections of these ports are limited by the Cryostat penetrations, no significant permanent damage to the vessel or structure from a seismic event is anticipated although some dampening, perhaps from the cryostat boots and feed-thrus might be implemented with good effect here.

-Areas where local bending + membrane stress may exceed yield, and areas of discontinuity or stress concentration were evaluated for fatigue. The primary cyclic loading (apart from the low number of pump-down/bakeout cycles) will be disruption loads. Assuming a conservative estimate of 5 disruption loads per day, over 10 years of operation, the cumulative number of cycles will be ~12,500. The stress range will vary based on location and residual stress. Specialty Metals/Huntington Alloys data indicates a fatigue life well in excess of 100 million cycles at the maximum anticipated cyclic stress for the base metal. For weld filler material, the literature indicates high margins for the cycle life and stress range anticipated. After accounting for shakedown, all stress excursions will fall well within the elastic range for all loading conditions considered.

-The creep-rupture properties at the maximum bakeout temperature of 400 C are extremely good for this material (Inconel 625) with rupture life in excess of 100,000 hrs (11.4 years) for the peak stress levels calculated. The accumulated vessel exposure to bakeout temperatures is not expected to exceed 10% of the rupture life (10,000 hrs).

ACKNOWLEDGMENTS

This work supported under DOE contract DE-AC02-76CH03073

REFERENCES

- [1] R Simmons, "Recent Progress in the Design, Fabrication, and R&D of NCSX", These proceedings.
- [2] P. Titus, M.Kalish "Seismic Analysis of The National Compact Stellarator Experiment (NCSX)", These Proceedings.

External Distribution

Plasma Research Laboratory, Australian National University, Australia
Professor I.R. Jones, Flinders University, Australia
Professor João Canalle, Instituto de Fisica DEQ/IF - UERJ, Brazil
Mr. Gerson O. Ludwig, Instituto Nacional de Pesquisas, Brazil
Dr. P.H. Sakanaka, Instituto Fisica, Brazil
The Librarian, Culham Laboratory, England
Mrs. S.A. Hutchinson, JET Library, England
Professor M.N. Bussac, Ecole Polytechnique, France
Librarian, Max-Planck-Institut für Plasmaphysik, Germany
Jolan Moldvai, Reports Library, Hungarian Academy of Sciences, Central Research Institute
for Physics, Hungary
Dr. P. Kaw, Institute for Plasma Research, India
Ms. P.J. Pathak, Librarian, Institute for Plasma Research, India
Ms. Clelia De Palo, Associazione EURATOM-ENEA, Italy
Dr. G. Grosso, Instituto di Fisica del Plasma, Italy
Librarian, Naka Fusion Research Establishment, JAERI, Japan
Library, Laboratory for Complex Energy Processes, Institute for Advanced Study,
Kyoto University, Japan
Research Information Center, National Institute for Fusion Science, Japan
Dr. O. Mitarai, Kyushu Tokai University, Japan
Dr. Jiengang Li, Institute of Plasma Physics, Chinese Academy of Sciences,
People's Republic of China
Professor Yuping Huo, School of Physical Science and Technology, People's Republic of China
Library, Academia Sinica, Institute of Plasma Physics, People's Republic of China
Librarian, Institute of Physics, Chinese Academy of Sciences, People's Republic of China
Dr. S. Mirnov, TRINITI, Troitsk, Russian Federation, Russia
Dr. V.S. Strelkov, Kurchatov Institute, Russian Federation, Russia
Professor Peter Lukac, Katedra Fyziky Plazmy MFF UK, Mlynska dolina F-2,
Komenskeho Univerzita, SK-842 15 Bratislava, Slovakia
Dr. G.S. Lee, Korea Basic Science Institute, South Korea
Institute for Plasma Research, University of Maryland, USA
Librarian, Fusion Energy Division, Oak Ridge National Laboratory, USA
Librarian, Institute of Fusion Studies, University of Texas, USA
Librarian, Magnetic Fusion Program, Lawrence Livermore National Laboratory, USA
Library, General Atomics, USA
Plasma Physics Group, Fusion Energy Research Program, University of California
at San Diego, USA
Plasma Physics Library, Columbia University, USA
Alkesh Punjabi, Center for Fusion Research and Training, Hampton University, USA
Dr. W.M. Stacey, Fusion Research Center, Georgia Institute of Technology, USA
Dr. John Willis, U.S. Department of Energy, Office of Fusion Energy Sciences, USA
Mr. Paul H. Wright, Indianapolis, Indiana, USA

The Princeton Plasma Physics Laboratory is operated
by Princeton University under contract
with the U.S. Department of Energy.

Information Services
Princeton Plasma Physics Laboratory
P.O. Box 451
Princeton, NJ 08543

Phone: 609-243-2750
Fax: 609-243-2751
e-mail: pppl_info@pppl.gov
Internet Address: <http://www.pppl.gov>